

Comparative Investigation on Thermally Sprayed Al_2O_3 , Al_2O_3 -13%(TiO_2) and Al_2O_3 -40%(TiO_2) Composite Coatings from Room to 400 °C Temperature

Deepak Kumar

Delhi Technological University <https://orcid.org/0000-0001-5411-9005>

Qasim Murtaza

Delhi Technological University

Pushendra Singh (✉ dr.psinghs@gmail.com)

Delhi Technological University

RS Walia

Punjab Engineering College Chandigarh

Research Article

Keywords: Coatings, Wear resistance, Friction, Flame spray process

Posted Date: August 3rd, 2021

DOI: <https://doi.org/10.21203/rs.3.rs-566802/v1>

License: © ⓘ This work is licensed under a Creative Commons Attribution 4.0 International License.

[Read Full License](#)

Version of Record: A version of this preprint was published at Surface Topography: Metrology and Properties on March 3rd, 2022. See the published version at <https://doi.org/10.1088/2051-672X/ac5a75>.

Abstract

The aim of this research is to study the comparative wear behaviour of pure Al_2O_3 with varying TiO_2 content due to the high demand in the industry for high temperature applications such as the automotive industry (piston ring and liner), petrochemicals industry (pump sleeves) and textile industry tools which require the hard bearing surface, abrasion resistance and particle corrosion at the temperature of up to 400°C . In the present study, three coatings of Al_2O_3 , Al_2O_3 -13%(TiO_2) and Al_2O_3 -40%(TiO_2) composite coatings were deposited by the thermally flame spray process. The comparative wear behaviour of the Al_2O_3 - TiO_2 coatings has been studied under high temperature of up to 400°C using a high temperature tribometer at a constant load of 40N. Before the wear test, the mechanical properties of the coated samples such as microhardness and surface roughness were studied. The morphological analysis was determined by field emission scanning electron microscope, elemental dispersion spectroscopy and X-ray powder diffraction techniques. The results reveal that specific wear rate decreases with a rise in temperature for all the deposited coating except Al_2O_3 coating at 400°C . The friction coefficient of deposited three alumina based coatings is decreasing with the increasing temperature. The research reveals that the Al_2O_3 -40% TiO_2 coating has the highest wear resistance properties as well as a low coefficient of friction due to its low hardness and high adhesion properties. For Al_2O_3 -40% TiO_2 coating the measured values of specific wear rate varying from $0.034567 \times 10^{-3} \text{ mm}^3/\text{Nm}$ to $0.014581 \times 10^{-3} \text{ mm}^3/\text{Nm}$ and the average values of coefficient friction ranging from 0.7284 to 0.3901 as temperature varying from room temperature to 400°C . In the worn out surface of deposited coatings, brittle fracture and abrasive wear behaviour were observed from room temperature to 400°C .

1. Introduction

Thermally sprayed ceramic coatings have been extensively used for enhancement of wear repairing as well as corrosion resistance at high temperature applications like in textile industry tools (thread grinding and ridge thread break)[1]. The Al_2O_3 - TiO_2 ceramic coatings are appropriate for applications such as the automotive industry (piston ring and liner), petrochemicals industry (pump sleeves) and shipboard and marine application[2, 3]. The application is for hydraulic components such as impellers, blowers and pump where these parts are damaged by solid particle on the surfaces[4, 5].

There is an increasing demand for the development of high temperature protective coatings with a low friction coefficient and desired wear resistance properties under various severe conditions. Ceramic coatings that hold exceptional chemical and physical properties can be deposited on the surface area of the industrial components to effectively enhance their wear properties [6, 7]. Many investigations have considered that Al_2O_3 - TiO_2 based ceramic coating shows less porosity, high hardness, high fracture toughness, excellent high temperature corrosion and wear resistance coating [8, 9].

Al_2O_3 with high hardness (15–19 GPa) and high mechanical strength (300–630 MPa) is one of the capable material for high temperature application [10, 11]. It has been reported that Al_2O_3 ceramic

coatings have high wear and corrosion resistant properties. On the other side TiO_2 ceramic coatings material possess excellent properties with compressive strength and high hardness (9330–10290 MPa) and (630–3675 MPa) respectively and also have good adhesion properties [12, 13]. Therefore, the accumulation of TiO_2 in Al_2O_3 coatings was found to be an effective way to enhance the wear resistance property of the coating at elevated temperature. It is because of the low melting point as well as high adhesion properties of TiO_2 which can easily be inserted into the pores between Al_2O_3 particles (Yilmaz 2007). Therefore, the mixing of TiO_2 and Al_2O_3 ceramic coating material reveals different excellent properties like low porosity, high mechanical strength and excellent wear and corrosion resistance [14, 15].

Previous studies have revealed that the microstructure and characteristic of the deposited coating are influenced not only by the parameters of the feed powder but also through the wear test conditions such as load, lubrication environment and temperature [16]. Al_2O_3 - TiO_2 coatings deposited from thermally flame spray methods from conventional or nano-structure and the agglomerated feedstock powder were thoroughly investigated [17–19]. Vicent et al [20] investigated the effect of size particle on microstructure and mechanical properties of the Al_2O_3 - TiO_2 coatings. Comparative investigation of Al_2O_3 - TiO_2 coatings in terms of different depositing technique and their tribological properties at room temperature were studied [21, 22]. Kusoglu et al [23] investigated the wear behaviour of flame sprayed Al_2O_3 - TiO_2 coatings at room temperature. Lin et al [24] studied the tribological properties of pure Al_2O_3 and Al_2O_3 -3% TiO_2 coatings up to temperature 600°C. It states that wear properties were improved as temperature rose. Although, previous investigations were restricted to wear resistance at room temperature and other deposition parameters. Whereas the analysis of wear behaviour is equally important at high temperature as per the current scenario of industry.

Stainless steel (SS 304) material is generally used for heat exchangers, boiler, aerospace applications such as rocket engines, exhaust pipes, and marine engineering [25, 26]. These materials have high heat resistance, high or excellent strength, low-density properties, high toughness at high temperatures. However, the properties of SS 304 material resistance to external impacts are insufficient/limited when confronted with high working conditions. Mainly in wear and corrosion at high temperature could lead to severe material failure, which is the main challenge for the manufacturing process [27, 28]. The hardness of the components made of stainless steel (SS) not have desired hardness (180–200 HV) and have a high wear rate during sliding wear under severe conditions [29]. The high wear rate of components in different units like in thermal power plant, textile industries, etc. directly impacts the productivity of the industries. Minimizing the wear would directly affect reducing the cost of components and reduce the shutdown of machineries [30]. To overcome the above stated problem, the composite coating of alumina based material by thermally sprayed technique is one of the possible solution and need current scenario as per the industrial aspects [31, 32].

The purpose of this research is to focus on the study of the wear behaviour of pure Al_2O_3 with varying TiO_2 content due to the high demand in the industry for high temperature applications which require the

hard bearing surface, abrasion resistance and particle corrosion at temperature of upto 400°C [33, 34]. In the present study thermally flame sprayed deposition technique has been used to deposit Al₂O₃ based composite coating. Since it has certain advantages like low cost, easy to handle, and most importantly, it is more adaptable to manufacturing processes with sort series. The main fuel gas used in the flame spray process is acetylene, which is combined with oxygen to produce high combustion temperatures and particle temperatures of over 2600°C[35]. The obtained temperature is sufficient for melting the powder particle and deposit on the substrate. Therefore, three different types of coatings with varying ratio of TiO₂, as-sprayed Al₂O₃, Al₂O₃ -13%(TiO₂) and Al₂O₃ -40%(TiO₂) were obtained by the flame spray process. The deposited coating was further investigated for a comparative study of coating morphology and wear behaviour at a high temperature of up to 400°C.

2. Material And Methods

2.1 Substrate Material

Austenitic stainless steel of grade 304 is used for elevated temperature applications. This steel was preferred as the substrate material in the present article. The chemical composition of the substrate is provided in Table 1. The circular plate of diameter 100mm and thickness 3 mm was taken from the selected substrate material.

Table 1
Nominal chemical composition of substrate (steel of grade 304 (wt %))[36].

Grade	Cr	Ni	Mn	N max.	S max.	C max.	Si max.	P max.	Fe
304	18-20	8-10	2	.10	.03	.08	.75	.045	Balanced

2.2 Coating Deposition

Commercially available Al₂O₃, Al₂O₃ -13% (TiO₂) and Al₂O₃ -40%(TiO₂) ceramic powders were used for comparison of wear behaviour at high temperature in this article. The composition details of the composite powders are given in Table 2. These ceramic powders were deposited on the given base material samples with the help of the flame spray process. The details of the coating parameters used for the deposition of the composite powders are given in Table 3 and the actual and schematic diagram of the thermally flame spray process is shown in Fig. 1. The given samples prior to coating deposition were grit blasted on the exposed surface. Alumina grit was used for grit blasting to increase the surface roughness to get desired coating adhesion. The uncoated substrate, after grit blasted substrate and coated the substrate of coatings are shown in Fig. 2.

Table 2
Composition details of composite powders.

Composite Powders	Company	Morphology	Manufacturing Method	Particle Size (µm)
Al ₂ O ₃	H.C. Strack	Irregular	Fused and irregular	-45 + 10
Al ₂ O ₃ -13%TiO ₂	H.C. Strack	Mixed Ellipsoid/ elongated	Fused and irregular	-45 + 10
Al ₂ O ₃ -40%TiO ₂	H.C. Strack	Angular	Fused and irregular	-45 + 10

The morphological study of powders was analyzed with the help of a finite electron scanning electron microscope (FESEM) (Carl Zeiss, from Indian Instrumentation Centre in Indian Institute of Technology, Roorkee, India). The electron dispersion spectroscopy (EDS) analysis was studied to authenticate the presence desired element in the composite powders. The FESEM micrographs and EDS analysis of powders are shown in Fig. 3. The investigation of the phases composition present in the obtained coatings was tested by X-ray diffraction (XRD) (DTU, New Delhi) and analyzed with the help of software Xpert Highscore Plus. The morphological study of the coated sample and its cross-sectional area were analyzed by FESEM before and after the friction and wear test. The microhardness and surface roughness of the coatings were also reported.

Table 3
Coating parameter used for flame spray deposition.

Oxygen flow rate	Acetylene Flow rate	Spraying distance	Nitrogen carrier flow rate	Oxygen Pressure	Acetylene Pressure	Nitrogen carrier pressure
45 NLPM	26 NLPM	75 mm	7 NPLM	2.4 bar	2.1 bar	4 bar

2.3 Friction and Wear Test

The friction and wear experimentation was carried out at constant sliding velocity 1m/s and load 40N on duccon high temperature tribometer (Delhi Technological University, New Delhi, India) according to ASTM G99 standard as shown in Fig. 4. The coated steel plate was mounted on high temperature tribometer and the pin of diameter 8 mm of material similar to base material was used as the counter body. The experiment parameters set for friction and wear test for a coated steel plate are given in Table 4. The acquisition system connected to the tribometer was used to feed the given parameters. The coefficient of friction and wear depth curve of the experimentation were taken with the system connected to the high temperature tribometer and specific wear rate were calculated using the Archands equation.

Table 4
Parameters set for friction and wear test for a coated steel plate.

S.No.	Track Diameter (mm)	Speed (rpm)	Sliding Distance (m)	Temperature (°C)	Load (N)
1	20	955	1000	25	40
2	30	636	1000	100	40
3	40	477	1000	200	40
4	50	382	1000	400	40

3. Result And Discussion

3.1 Coating Characterization

The morphology of the three different ceramic coatings were examined with the help of the FE-SEM as shown in Fig. 5. The FESEM image of Fig. 5 (a) is Al_2O_3 coating, Fig. 5 (b) is Al_2O_3 -13% (TiO_2) coating and Fig. 5 (c) is Al_2O_3 -40% (TiO_2) coating. The examination reveals that coatings possess laminar splats, minor micro-cracks and the partially melted region. Figure 5 (a) and (b) show a few pores which are comparatively more than shown in Fig. 5 (c). Micro-pore and interconnected pores are evident as dark regions in the coatings in Fig. 5 (b). The laminar cracks got generated on the coating surface due to the high temperature flame i.e. that regions were highly exposed to the heat generated by the flame spray torch. During the flame process, powder particles are behaving differently. Some power created a completely melted region while some created partially melted, this may be due to the distribution in the powder particle and also temperature distribution in flame spray torch.

In flame sprayed, the particles were melted due to high temperature flames produced in the gun. These melted droplets accelerated and strike towards the substrate at high speed to form the micro-level laminar structured and dense coating. Due to the high speed of the flame and distance between the substrate and gun, some powder particles were not fully melted during the flying and created the partially melted region on the substrate (see in Fig. 5a). Besides, a few micro cracks and pores were also developed at the time of coating deposition. The cross sectional images of the deposited coating were also taken with FESEM micrographs and element mapping as shown in Fig. 6. The thickness of the different deposited coating ranges from 148 to 152 μm i.e. for Al_2O_3 coating is 148.8 μm , Al_2O_3 -13% TiO_2 is 152.1 μm and Al_2O_3 -40% TiO_2 is 151.19 μm . The element mapping reveals the evenly distribution of the powder materials on the surface of the deposited coatings.

The EDS results of the coatings are provided in Fig. 7. It shows the mass percentage of the different elements of the coatings. The XRD pattern of the different deposited coatings was shown in Fig. 8. In Al_2O_3 coating, the XRD pattern shows the presence of some γ - Al_2O_3 and alpha α - Al_2O_3 phases in the deposited coating. The presence of α - Al_2O_3 was caused by the partially melted pf the powders in the

flame spray, as confirmed above in the microstructure. In the 13% TiO₂ coating, the pattern shows some rutile TiO₂ reacted with Al₂O to form Al₂TiO₅ because of the high temperature during flame spraying. In 40% TiO₂, the major phase was rutile tialite Al₂TiO₅. The tialite phase was formed as a consequence of the reaction between the spraying flame of Al₂O₃ and TiO₂ particle.

The microhardness of the deposited coating with varying TiO₂ content is tested using a micro vickers hardness tester and shown in Fig. 9. The value of the microhardness is measured at load 300 gm with a dwell time of 10 seconds. The measured value is taken at an average of five different reading with the same conditions. The microhardness values for Al₂O₃ is 913.30HV, Al₂O₃ 13% TiO₂ is 900.15 HV and for 40% TiO₂ is 742.17 HV. The Al₂O₃ + 13% TiO₂ has the highest average microhardness value. The surface roughness of the deposited coatings was obtained. The measured values are 5.3 μm for Al₂O₃, 6.3 μm for Al₂O₃-13%TiO₂ and 6 μm for Al₂O₃-40%TiO₂.

3.2 Specific Wear Rate

The standard wear test equation for specific wear rate (also known as wear coefficient) is often used in categorizing the resistance to contact wear [37, 38]. Expression for calculating the wear coefficient is given in Eq. 1.

$$K = \frac{V_w}{W \cdot s} \quad (1)$$

Where, K - specific wear rate (mm³/Nm)

V_w - Wear volume (mm³)

W - Load (N)

s - Sliding distance (m)

These wear coefficients are reflected as system dependent quantities i.e. (i) contact materials (ii) surroundings and systems and (iii) operational condition [39]. Also, the wear behaviour of the coatings is subjective to various elements such as porosity, hardness and fracture toughness. These properties result in lower wear rate whereas lower porosity indicates the higher rate of wear of the coatings [40].

The specific wear rate of the deposited Al₂O₃, Al₂O₃ -13%(TiO₂) and Al₂O₃ -40%(TiO₂) ceramic coatings is taken at different temperature of 25 °C, 100 °C, 200 °C and 400 °C at constant load 40N and sliding velocity 1m/s is illustrated in Fig. 10. The measured value of specific wear rate for Al₂O₃ deposited coatings are 0.063684*10⁻³ mm³/Nm at temperature 25°C, 0.045265*10⁻³ mm³/Nm at 100 °C, 0.034228*10⁻³ mm³/Nm at 200 °C. But it slightly increases to 0.072183*10⁻³ mm³/Nm at 400 °C. Whereas in Al₂O₃-13%TiO₂ coating the obtained values are 0.040595 *10⁻³ mm³/Nm, 0.030219 *10⁻³ mm³/Nm, 0.024618 *10⁻³ mm³/Nm and 0.026756*10⁻³ mm³/Nm with different temperature of 25 °C,

100 °C, 200 °C and 400 °C respectively. In case of Al₂O₃-40%TiO₂ the values are decreasing 0.034567*10⁻³ mm³/Nm to 0.014581*10⁻³ mm³/Nm with temperature of 25 °C, 100 °C, 200 °C and 400 °C respectively. It is visible (Fig. 10) that the specific wear rate is continuously decreasing with the successive rise in temperature except in the case of Al₂O₃ coating at 400 °C. From the above discussion, For Al₂O₃ coating, it is clear that the wear coefficient is decreasing up to 200 °C and suddenly increases at 400 °C due to chippings or spalling from the substrate[41]. The removed splats are broken into more modest hard particles and entrapped in the deeper crater due to continual action sliding cycles. The trapping of hard particles in crater increases the applied stress on the worn surface. It causes the dynamic of the contacting bodies to change, potentially resulting in a high specific wear rate[42].

It is clear from Fig. 10, at 400 °C for Al₂O₃ deposited coating the highest specific wear rate is observed i.e. this 0.072183*10⁻³ mm³/Nm. The wear properties depend upon the debris characteristics and the contact temperature. This effect could also be explained due to the deformation of the protective layer of the coating. The deposited coating has been plastically deformed and appears to be enough ploughed. This deformation and ploughing results in a large detachment from the substrate. Similar results were also reported about the specific wear rate of Al₂O₃ coatings rise when the temperature is raised to 400 °C [43]. Tetsuya Senda et al. [44] found that at elevated temperature, the grain size has a significant impact on the wear resistance behaviour of alumina coating. The larger wear grooves of nanostructure coating also confirm the increase in wear rate at 25 °C, 100 °C, 200 °C and 400 °C, respectively.

For Al₂O₃-13%TiO₃, the decrease in the wear coefficient is observed with the increase in temperature of up to 200 °C. However, at 400 °C, Al₂O₃-13%TiO₃ coating shows a slightly increasing trend in specific wear rate which is much lesser than pure Al₂O₃ coating at the same temperature. This is due to the less spalling/chipping formation in the Al₂O₃-13%TiO₃ coating on the substrate. Whereas a similar specific wear rate trend was observed for Al₂O₃-40%TiO₃ coating till 200 °C. However, at 400 °C Al₂O₃-40%TiO₃ coating shows a gradually decreasing trend in specific wear rate. The addition of TiO₂ content in Al₂O₃ composite coating results in the drop of hardness of the coating which affects the material loss of the coating [45]. Subsequently, it results in added adhesive mode when compared with pure Al₂O₃. Hence, the adhesive wear mechanism is consistent and dominant as well [46].

All the even and compacted areas spread in the wear track are attained at 400°C and 200°C as well, but at room temperature, micro-traces of wear scars were observed. At room temperature 100°C, 200°C and 400°C, respectively, conventional wear scars of microstructured coating were formed. At 400°C, there are many smooth and compact patches distributed in the wear scars; a few patches are dispersed at 200°C and 100°C. It can be deduced that as a temperature rises, the area of this smooth and compacted zone in the wear scar grows.

3.3 Coefficient of Friction

Figure 11 depicts the evolution of the coefficient of friction (COF) trend of Al_2O_3 based ceramic coatings at a constant load of 40 N under the influence of four levels of variable temperatures (25°C, 100°C, 200°C and 400°C) for a sliding distance of 1000m. It can be seen from Fig. 11 that the COF of pure Al_2O_3 based coating is decreasing with increasing temperature from 25°C to 200°C. While COF was maximum of 0.92 at the maximum operating temperature of 400°C, this may be due to chippings or spalling of the coating from the substrate while rubbing or sliding.

For Al_2O_3 -13% TiO_2 coating the COF is decreasing with increasing the temperature i.e. the obtained values are 0.921, 0.795, 0.697 and 0.5863 with temperature 25°C, 100°C, 200°C and 400°C respectively. Similar trends were also seen for Al_2O_3 -40% TiO_2 coating where COF ranges from 0.7284 to 0.3901 and temperature ranges from 25°C to 400°C respectively. Hence, the coating Al_2O_3 -40% TiO_2 has less coefficient of friction as compared to the other two coatings i.e. Al_2O_3 and Al_2O_3 -13% TiO_2 .

The Al_2O_3 - TiO_2 coatings and counter body react in a tribo-chemical nature which is controlled and results in the reduction of the COF. The continuous reduction in the friction coefficient can be linked to the actual contact area between the scouring surfaces. At the initial stage of the sliding, the asperities of the surface resist the sliding speed. Meanwhile, the friction causes the eradication of few asperities. The eradicated asperities would result in a change of applied stress on the worn-out surface. Thereby changing the mechanism of two or three body abrasions involved in the wear process[47].

The decrease in COF is due to the development of the oxide layer on the coating surface which acts as a protective layer. Therefore, the sticking tendency of wear debris and material shear strength gets reduced with the increase of the operating temperature. So, the contact temperature produces softening and melting of the wear debris. These similar trends reported about the tribological properties of Al_2O_3 - TiO_2 coatings are also highly determined by test environments, such as temperature and contact load [48, 49]. The wear of deposited Al_2O_3 - TiO_2 coatings is decreased in the presence of absorbed environmental moisture [50]. The coefficient of friction decreases with the surge in the operating temperature due to the development of tribo-layer at higher temperatures subsequently the tribo-layer is dense and even, therefore it has a significant role in the reduction of the coefficient of friction [51].

3.4 Wear Mechanism

The wear behaviour of Al_2O_3 - TiO_2 coatings was mainly affected by the microstructure, porosity, micro cracks and mechanical properties like fracture toughness, hardness. Many researchers reported different wear mechanism of the alumina based composite coating. Figure 12A, D, G, J reports the wear behaviours of the Al_2O_3 based ceramic coatings at the temperature of 25°C, 100°C, 200°C and 400°C respectively with a constant load of 40N and sliding distance of 1000m. At 25°C the Al_2O_3 coating shows the abrasion wear due to the more roughness and larger surface contact between the substrate and the counter body. While temperature is increasing up to 200°C the wear track is showing a decreasing trend. This is due to the fact of higher temperature stability of the coating at 200–300°C. Another evidence for the mild wear of the coating owing to the existence of oxygen in the wear track results in oxidation of fine

wear debris, their accumulation and subsequent development of tribo-film. But at 400°C Al₂O₃ coating showed the poor wear resistance detachment of the coating particles from the substrate. As there was a complete presence of Al₂O₃ content in the top layer of the deposited coating.

As per FESEM micrographs of the coatings Al₂O₃-13% TiO₂ at 200 and 400°C, ploughing and plastic deformation marks were observed on the worn surfaces along with areas of brittle fracture. The mechanism appears to be similar for all the wear surfaces. The major difference has been observed only in the brittle fracture areas caused due to ductility and cohesion of the coating. Furthermore, in Al₂O₃-40%TiO₂, the worn surfaces indicated that the material is frequently detached by ploughing and brittle fracture. The main type of wear in the Al₂O₃-TiO₂ coating sliding against stainless steel is a brittle fracture and abrasive behaviour [22]. Initially, the wear mechanism is effectively caused by abrasion and after the bond formation with the substrate, it would lose material by adhesion [14, 52, 53]. Marin et al., [54] stated third body wear scars present inside the wear track visible on the surface of the coating.

Different types of morphologies can be identified on the worn surfaces of Al₂O₃-TiO₂ coating after wear tests under variable temperature and constant load (i) material removal for delamination of the surface layers, with pits and micro-cracks randomly distributed over the wear track (Fig. 12), and (ii) metallic film deposition (Fig. 12h). In the first case, during dry sliding, micro-cracks and dislocated networks may yield wear debris as detected inside pits. The wear particles are trapped in the contact interface and are subjected to continuous fracture, distortion or chemical reaction, producing micro-sized powders[55].

Whereas wear mechanism in Al₂O₃ with varying percentage of TiO₂ coating wears scars, wear track with the flattened surface, minor cracks and severe abrasion, micro brittle fracture mostly reported in the researchers[56, 57]. Oge [58] observed the fatigue-induced surface cracks and consequent spallation arising due to the plastic deformation of the coating. While at high temperature, Al₂O₃- TiO₂ shows the brittle fracture during sliding wear on the worn surface of the deposited coating at a temperature varying from 25°C to 400°C. This mainly occurs due to the desorption of the moisture at elevated temperature [59].

4. Conclusions

In the present paper Al₂O₃-TiO₂ based ceramic coatings were successfully coated by the thermally flame spray process. The objective of this research is to compare the different coatings and obtain the best wear resistance coating for high temperature applications. The wear behaviour of different coatings was studied out at four levels of temperatures (25 °C, 100 °C, 200 °C and 400 °C). Subsequently coated samples were characterized on the basis of morphological analysis and various mechanical properties. The findings in this research have drawn the following conclusions.

- The thermally flame spray coating exhibits a relatively dense lamellar microstructure with laminar splats, minor micro-cracks, partially melted region and few pores in the microstructure.
- The thickness of the deposited coatings ranges from 148- 152 µm.

- The $\text{Al}_2\text{O}_3+40\%\text{TiO}_2$ has shown the least microhardness value. The average microhardness values for Al_2O_3 coating is 913.30HV, $\text{Al}_2\text{O}_3-13\%\text{TiO}_2$ coating is 900.15 HV and for $40\%\text{TiO}_2$ coating is 742.17 HV.
- The specific wear rate of Al_2O_3 , $\text{Al}_2\text{O}_3-13\%(\text{TiO}_2)$ and $\text{Al}_2\text{O}_3-40\%(\text{TiO}_2)$ coatings determined were more in the initial stage, which decreases to a steady-state in the latter. The specific wear rate is decreasing with the increase in the temperature at a constant load and sliding distance. Whereas For Al_2O_3 coating, the wear coefficient suddenly increases at $400\text{ }^\circ\text{C}$ due to chippings or spalling from the substrate. This is because of the deformation and ploughing that causes the large detachment of coating particles from the substrate at high temperature.
- The friction coefficient of deposited three alumina based is decreasing with the increasing temperature. The decrease in the friction coefficient is governed by tribochemical reactions between alumina-based coatings and counter-body. There is a reduction in the sticking tendency of wear debris with increasing temperature and the formation of oxides is favoured as the contact layer.
- The main type of wear in Al_2O_3 based coatings sliding against stainless steel counter body is a brittle fracture and abrasive behaviour. Whereas wear mechanism in Al_2O_3 with varying percentage of TiO_2 coating wears scars, wear track with the flattened surface, minor cracks and severe abrasion. The fatigue-induced surface cracks and consequent spallation arises due to the plastic deformation of the coating.
- At high temperature, the coatings show the brittle fracture during sliding wear on the worn surface of the deposited coating at a temperature varying from $25\text{ }^\circ\text{C}$ to $400\text{ }^\circ\text{C}$.
- The $\text{Al}_2\text{O}_3-40\%\text{TiO}_2$ coating has high wear resistance properties as well as low coefficient of friction as compared to $\text{Al}_2\text{O}_3-13\%\text{TiO}_2$ coating and Al_2O_3 coating.

Declarations

Acknowledgement

The authors are grateful to the precision and manufacturing Laboratory (DTU, New Delhi, India) for performing the wear test experiments.

Funding - The current research was partly funded by Technical Education Quality Improvement Programme (TEQIP, DTU), the Government of India assisted by World Bank (Grand Order No. DTU/TEQIP-III/2019-20/369). This TEQIP funding was utilized for characterization of materials.

Conflicts of interest - The authors have no conflicts of interest to declare that are relevant to the content of this article. The authors have financial or proprietary interests in any material discussed in this article.

Availability of data and material - Not applicable.

Code availability - Not applicable.

Ethics approval - Not applicable.

Consent to participate - All authors participate and contribute in the current research work.

Consent to publication - The authors agree to publish the results of the current research work.

References

1. Liu Q, He T, Guo WY, et al (2019) Tribological behavior of SAPS sprayed Al₂O₃-TiO₂ and NiCr-Cr₃C₂ coatings under severe load conditions. *Surf Coatings Technol* 370:362–373. <https://doi.org/10.1016/j.surfcoat.2019.03.044>
2. Di Girolamo G, Brentari A, Blasi C, Serra E (2014) Microstructure and mechanical properties of plasma sprayed alumina-based coatings. *Ceram Int* 40:12861–12867. <https://doi.org/10.1016/j.ceramint.2014.04.143>
3. Gell M, Jordan EH, Sohn YH, et al (2001) Development-and-implementation-of-plasma-sprayed-nanostructured-ceramic-coatings_2001_Surface-and-Coatings-Technology.pdf. 147:48–54
4. Bandyopadhyay PP, Chicot D, Venkateshwarlu B, et al (2012) Mechanical properties of conventional and nanostructured plasma sprayed alumina coatings. *Mech Mater* 53:61–71. <https://doi.org/10.1016/j.mechmat.2012.05.006>
5. Mehar S, Sapate SG, Vashishtha N, Bagde P (2020) Effect of Y₂O₃ addition on tribological properties of plasma sprayed Al₂O₃-13% TiO₂ coating. *Ceram Int* 46:11799–11810. <https://doi.org/10.1016/j.ceramint.2020.01.214>
6. Singh R, Tiwari SK, Mishra SK (2012) Cavitation erosion in hydraulic turbine components and mitigation by coatings: Current status and future needs. *J Mater Eng Perform* 21:1539–1551. <https://doi.org/10.1007/s11665-011-0051-9>
7. Kumar Goyal D, Singh H, Kumar H, Sahni V (2012) Slurry erosion behaviour of HVOF sprayed WC-10Co-4Cr and Al₂O₃+13TiO₂ coatings on a turbine steel. *Wear* 289:46–57. <https://doi.org/10.1016/j.wear.2012.04.016>
8. Zavareh MA, Sarhan AADM, Razak BBA, Basirun WJ (2014) Plasma thermal spray of ceramic oxide coating on carbon steel with enhanced wear and corrosion resistance for oil and gas applications. *Ceram Int* 40:14267–14277. <https://doi.org/10.1016/j.ceramint.2014.06.017>
9. Cui C, Hou W (2014) Properties of Fe-based amorphous alloy coatings with Al₂O₃-13% TiO₂ deposited by plasma spraying. *Xiyou Jinshu Cailiao Yu Gongcheng/Rare Met Mater Eng* 43:2576–2579. [https://doi.org/10.1016/s1875-5372\(15\)60004-2](https://doi.org/10.1016/s1875-5372(15)60004-2)
10. Oh ST, Sando M, Niihara K (2001) Mechanical and magnetic properties of Ni-Co dispersed Al₂O₃ nanocomposites. *J Mater Sci* 36:1817–1821. <https://doi.org/10.1023/A:1017541112681>
11. Hemalatha K, Venkatachalapathy VSK, Alagumurthy N (2013) Processing and Synthesis of Metal Matrix Al₆₀₆₃/Al₂O₃ Metal Matrix Composite by Stir Casting Process. *J Eng Res Appl* www.ijera.com ISSN 3:2248–96221390

12. Salman KD, Hasan LK (2020) Dry sliding wear behavior of composite materials fabricated by powder metallurgy. *J Mech Eng Res Dev* 44:232–241
13. Mthisi A, Popoola API (2019) Influence of Al₂O₃ addition on the hardness and in vitro corrosion behavior of laser synthesized Ti-Al₂O₃ coatings on Ti-6Al-4V. *Int J Adv Manuf Technol* 100:917–927. <https://doi.org/10.1007/s00170-018-2785-0>
14. Wang Y, Jiang S, Wang M, et al (2000) Abrasive wear characteristics of plasma sprayed nanostructured alumina/titania coatings. *Wear* 237:176–185. [https://doi.org/10.1016/S0043-1648\(99\)00323-3](https://doi.org/10.1016/S0043-1648(99)00323-3)
15. Yang K, Li J, Wang QY, et al (2019) Effect of laser remelting on microstructure and wear resistance of plasma sprayed Al₂O₃-40%TiO₂ coating. *Wear* 426–427:314–318. <https://doi.org/10.1016/j.wear.2019.01.100>
16. Goberman D, Sohn YH, Shaw L, et al (2002) Microstructure development of Al₂O₃-13wt.%TiO₂ plasma sprayed coatings derived from nanocrystalline powders. *Acta Mater* 50:1141–1152. [https://doi.org/10.1016/S1359-6454\(01\)00414-1](https://doi.org/10.1016/S1359-6454(01)00414-1)
17. Berger LM, Sempf K, Sohn YJ, Vaßen R (2018) Influence of Feedstock Powder Modification by Heat Treatments on the Properties of APS-Sprayed Al₂O₃-40% TiO₂ Coatings. *J Therm Spray Technol* 27:654–666. <https://doi.org/10.1007/s11666-018-0716-0>
18. Arboleda JA, Serna CM, Cadavid E, et al (2018) Effect of flame spray deposition parameters on the microstructure of Al₂O₃ - 13 %TiO₂ coatings applied onto 7075 aluminum alloy. *Mater Res* 21:3–14. <https://doi.org/10.1590/1980-5373-MR-2018-0038>
19. Wu RR, Wang RF, Li QS, Zhao H Le (2018) Microstructure and Mechanical Properties of Al₂O₃ /7075. *Zhuzao/Foundry* 67:695–698
20. Vicent M, Bannier E, Carpio P, et al (2015) Effect of the initial particle size distribution on the properties of suspension plasma sprayed Al₂O₃-TiO₂ coatings. *Surf Coatings Technol* 268:209–215. <https://doi.org/10.1016/j.surfcoat.2014.12.010>
21. Utu ID, Marginean G, Hulka I, et al (2015) Properties of the thermally sprayed Al₂O₃-TiO₂ coatings deposited on titanium substrate. *Int J Refract Met Hard Mater* 51:118–123. <https://doi.org/10.1016/j.ijrmhm.2015.03.009>
22. Deng W, Li S, Hou G, et al (2017) Comparative study on wear behavior of plasma sprayed Al₂O₃ coatings sliding against different counterparts. *Ceram Int* 43:6976–6986. <https://doi.org/10.1016/j.ceramint.2017.02.122>
23. Kusoglu IM, Celik E, Cetinel H, et al (2005) Wear behavior of flame-sprayed Al₂O₃ -TiO₂ coatings on plain carbon steel substrates. *Surf Coatings Technol* 200:1173–1177. <https://doi.org/10.1016/j.surfcoat.2005.02.219>
24. Lin X, Zeng Y, Ding C, Zhang P (2004) Effects of temperature on tribological properties of nanostructured and conventional Al₂O₃-3 wt.% TiO₂ coatings. *Wear* 256:1018–1025. [https://doi.org/10.1016/S0043-1648\(03\)00541-6](https://doi.org/10.1016/S0043-1648(03)00541-6)

25. Yang X, Liu M, Liu Z, et al (2020) Failure analysis of a 304 stainless steel heat exchanger in liquid sulfur recovery units. *Eng Fail Anal* 116:104729. <https://doi.org/10.1016/j.engfailanal.2020.104729>
26. Kanwal S, Ali NZ, Hussain R, et al (2020) Poly-thiourea formaldehyde based anticorrosion marine coatings on Type 304 stainless steel. *J Mater Res Technol* 9:2146–2153. <https://doi.org/10.1016/j.jmrt.2019.12.045>
27. Wang QY, Bai SL, Liu Z De (2014) Surface characterization and erosion-corrosion behavior of Q235 steel in dynamic flow. *Tribol Lett* 53:271–279. <https://doi.org/10.1007/s11249-013-0265-0>
28. Zhou J, Sun K, Huang S, et al (2020) Fabrication and property evaluation of the Al₂O₃-TiO₂ composite coatings prepared by plasma spray. *Coatings* 10:1–15. <https://doi.org/10.3390/coatings10111122>
29. Zhang L, Lu JZ, Luo KY, et al (2013) Residual stress, micro-hardness and tensile properties of ANSI 304 stainless steel thick sheet by fiber laser welding. *Mater Sci Eng A* 561:136–144. <https://doi.org/10.1016/j.msea.2012.11.001>
30. Majumdar A, Jana S (2001) Glass and glass-ceramic coatings, versatile materials for industrial and engineering applications. *Bull Mater Sci* 24:69–77. <https://doi.org/10.1007/BF02704843>
31. Toma FL, Potthoff A, Berger LM, Leyens C (2015) Demands, Potentials, and Economic Aspects of Thermal Spraying with Suspensions: A Critical Review. *J Therm Spray Technol* 24:1143–1152. <https://doi.org/10.1007/s11666-015-0274-7>
32. Tingaud O, Bertrand P, Bertrand G (2010) Microstructure and tribological behavior of suspension plasma sprayed Al₂O₃ and Al₂O₃-YSZ composite coatings. *Surf Coatings Technol* 205:1004–1008. <https://doi.org/10.1016/j.surfcoat.2010.06.003>
33. Abdel Aziz M, Mahmoud TS, Zaki ZI, Gaafer AM (2006) Heat treatment and wear characteristics of Al₂O₃ and TiC particulate reinforced AA6063 Al alloy hybrid composites. *J Tribol* 128:891–894. <https://doi.org/10.1115/1.2345416>
34. Tirth V (2018) Dry Sliding Wear Behavior of 2218 Al-Alloy-Al₂O₃(TiO₂) Hybrid Composites. *J Tribol* 140:. <https://doi.org/10.1115/1.4037697>
35. Habib KA, Saura JJ, Ferrer C, et al (2006) Comparison of flame sprayed Al₂O₃/TiO₂ coatings: Their microstructure, mechanical properties and tribology behavior. *Surf Coatings Technol* 201:1436–1443. <https://doi.org/10.1016/j.surfcoat.2006.02.011>
36. Li Y, Shen Y, Hung CH, et al (2018) Additive manufacturing of Zr-based metallic glass structures on 304 stainless steel substrates via V/Ti/Zr intermediate layers. *Mater Sci Eng A* 729:185–195. <https://doi.org/10.1016/j.msea.2018.05.052>
37. Holmberg K, Mathews A (1994) Coatings tribology: a concept, critical aspects and future directions. *Thin Solid Films* 253:173–178. [https://doi.org/10.1016/0040-6090\(94\)90315-8](https://doi.org/10.1016/0040-6090(94)90315-8)
38. Kumar D, Pandey SM, Murtaza Q, et al (2021) Tribological Analysis of Increasing Percentage of CrC Content in Composite Coating by Atmospheric Plasma Spray Technique. 99–113. https://doi.org/10.1007/978-981-15-4550-4_6

39. Singh SK, Chattopadhyaya S, Pramanik A, Kumar S (2018) Wear behavior of chromium nitride coating in dry condition at lower sliding velocity and load. *Int J Adv Manuf Technol* 96:1665–1675. <https://doi.org/10.1007/s00170-017-0796-x>
40. Rong J, Yang K, Zhao H, et al (2016) Tribological performance of plasma sprayed Al₂O₃–Y₂O₃ composite coatings. *Surf Coatings Technol* 302:487–494. <https://doi.org/10.1016/j.surfcoat.2016.06.053>
41. Małecka J (2012) Effect of an Al₂O₃ coating on the oxidation process of a γ -TiAl phase based alloy. *Corros Sci* 63:287–292. <https://doi.org/10.1016/j.corsci.2012.06.009>
42. Thirugnanasambantham KG, Natarajan S (2016) Mechanistic studies on degradation in sliding wear behavior of IN718 and Hastelloy X superalloys at 500 °C. *Tribol Int* 101:324–330. <https://doi.org/10.1016/j.triboint.2016.04.016>
43. Senda T, Drennan J, McPherson R (1995) Sliding Wear of Oxide Ceramics at Elevated Temperatures. *J. Am. Ceram. Soc.* 78:3018–3024
44. Senda T, Yasuda E, Kaji M, Bradt RC (1999) Effect of grain size on the sliding wear and friction of alumina at elevated temperatures. *J Am Ceram Soc* 82:1505–1511. <https://doi.org/10.1111/j.1151-2916.1999.tb01948.x>
45. Leszek Ł, Michalak M, Walczak M (2021) Influence of 13 wt % TiO₂ content in alumina-titania powders on microstructure, sliding wear and cavitation erosion resistance of APS sprayed coatings *Surface & Coatings Technology* Influence of 13 wt % TiO₂ content in alumina-titania powders on microstr. <https://doi.org/10.1016/j.surfcoat.2021.126979>
46. Szala M, Łatka L, Awtoniuk M, et al (2020) Neural modelling of aps thermal spray process parameters for optimizing the hardness, porosity and cavitation erosion resistance of Al₂O₃-13 wt% TiO₂ coatings. *Processes* 8:1–15. <https://doi.org/10.3390/pr8121544>
47. Vargas F, Ageorges H, Fournier P, et al (2010) Mechanical and tribological performance of Al₂O₃-TiO₂ coatings elaborated by flame and plasma spraying. *Surf Coatings Technol* 205:1132–1136. <https://doi.org/10.1016/j.surfcoat.2010.07.061>
48. Ravikiran A, Nagarajan VS, Biswas SK, Bai BNP (1995) Effect of Speed and Pressure on Dry Sliding Interactions of Alumina against Steel. *J Am Ceram Soc* 78:356–364. <https://doi.org/10.1111/j.1151-2916.1995.tb08808.x>
49. Andersson P, Blomberg A (1993) Alumina in unlubricated sliding point, line and plane contacts. *Wear* 170:191–198. [https://doi.org/10.1016/0043-1648\(93\)90240-M](https://doi.org/10.1016/0043-1648(93)90240-M)
50. Oladijo OP, Popoola API, Booi M, et al (2020) Corrosion and mechanical behaviour Of Al₂O₃.TiO₂ composites produced by spark plasma sintering. *South African J Chem Eng* 33:58–66. <https://doi.org/10.1016/j.sajce.2020.05.001>
51. Lu L, Ma Z, Wang FC, Liu YB (2013) Friction and wear behaviors of Al₂O₃-13 wt%TiO₂ coatings. *Rare Met* 32:87–92. <https://doi.org/10.1007/s12598-013-0008-2>
52. Liu Y, Fischer TE, Dent A (2003) Comparison of HVOF and plasma-sprayed alumina/titania coatings - Microstructure, mechanical properties and abrasion behavior. *Surf Coatings Technol* 167:68–76.

[https://doi.org/10.1016/S0257-8972\(02\)00890-3](https://doi.org/10.1016/S0257-8972(02)00890-3)

53. Krishnamurthy N, Prashanthareddy MS, Raju HP, Manohar HS (2012) A Study of Parameters Affecting Wear Resistance of Alumina and Yttria Stabilized Zirconia Composite Coatings on Al-6061 Substrate. *ISRN Ceram* 2012:1–13. <https://doi.org/10.5402/2012/585892>
54. Marin E, Lanzutti A, Fedrizzi L (2013) Tribological properties of nanometric atomic layer depositions applied on AISI 420 stainless steel. *Tribol Ind* 35:208–216
55. Luo H, Song P, Khan A, et al (2017) Alternant phase distribution and wear mechanical properties of an Al₂O₃-40 wt%TiO₂ composite coating. *Ceram Int* 43:7295–7304. <https://doi.org/10.1016/j.ceramint.2017.03.029>
56. Deshpande P V., Vadiraj A, Manivasagam G, et al (2013) Lubricated sliding wear behaviour of Al₂O₃-13TiO₂ coatings. *Surf Eng* 29:447–454. <https://doi.org/10.1179/1743294413Y.0000000135>
57. Yilmaz Ş (2009) An evaluation of plasma-sprayed coatings based on Al₂O₃ and Al₂O₃-13 wt.% TiO₂ with bond coat on pure titanium substrate. *Ceram Int* 35:2017–2022. <https://doi.org/10.1016/j.ceramint.2008.11.017>
58. Öge M, Kucuk Y, Gok MS, Karaoglanli AC (2019) Comparison of dry sliding wear behavior of plasma sprayed FeCr slag coating with Cr₂O₃ and Al₂O₃-13TiO₂ coatings. *Int J Appl Ceram Technol* 16:2283–2298. <https://doi.org/10.1111/ijac.13273>
59. V.V. Narulkar , S. Prakash and KC (2008) Effects of Temperature on Tribological Properties of Al₂ O₃ - TiO₂ Coating. *Def Sci J* 58:582–587. <https://doi.org/https://doi.org/10.14429/dsj.58.1680>

Figures

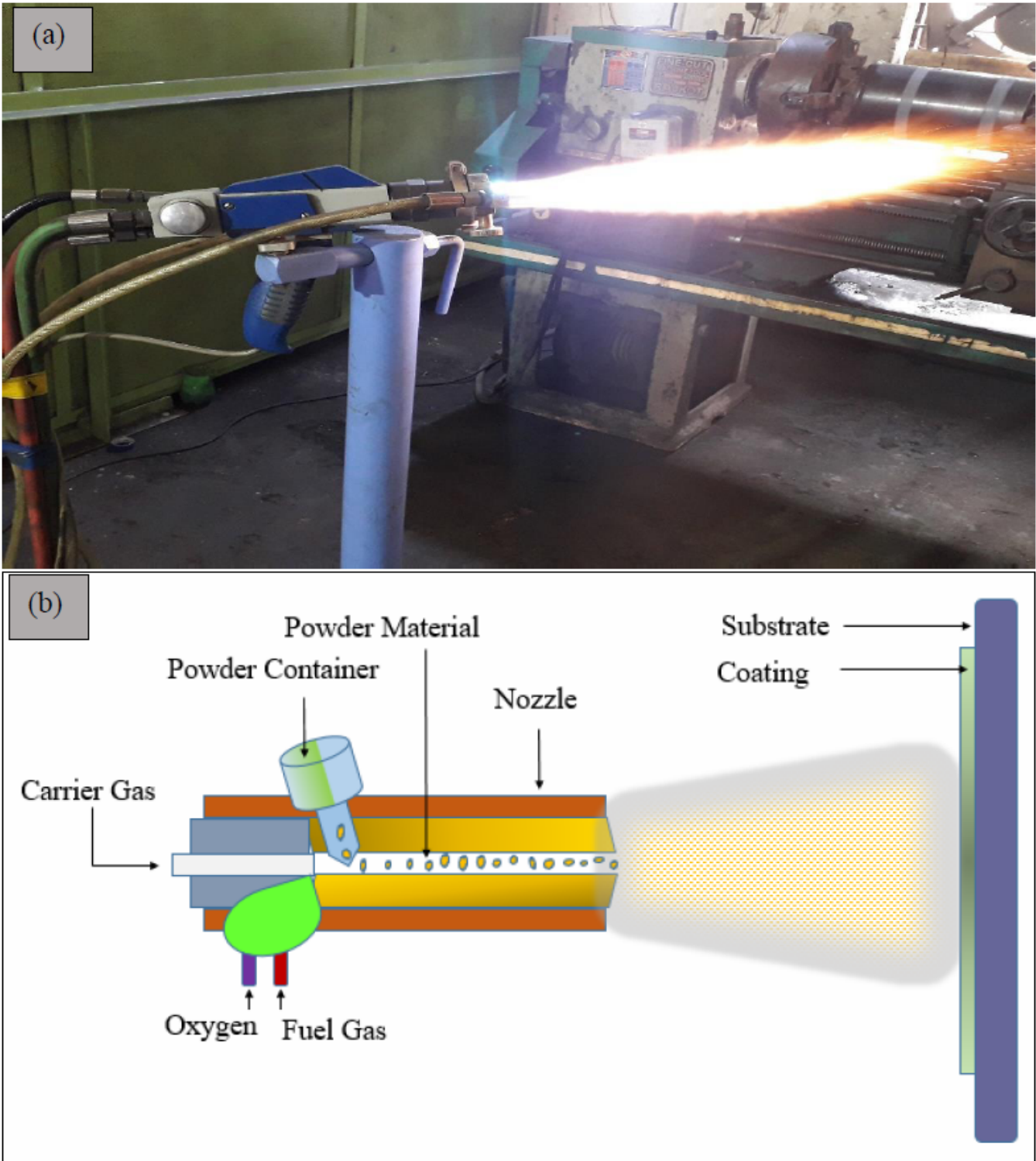


Figure 1

Thermally flame spray equipment : (a) actual image of the equipment (b) schematic diagram of equipment.

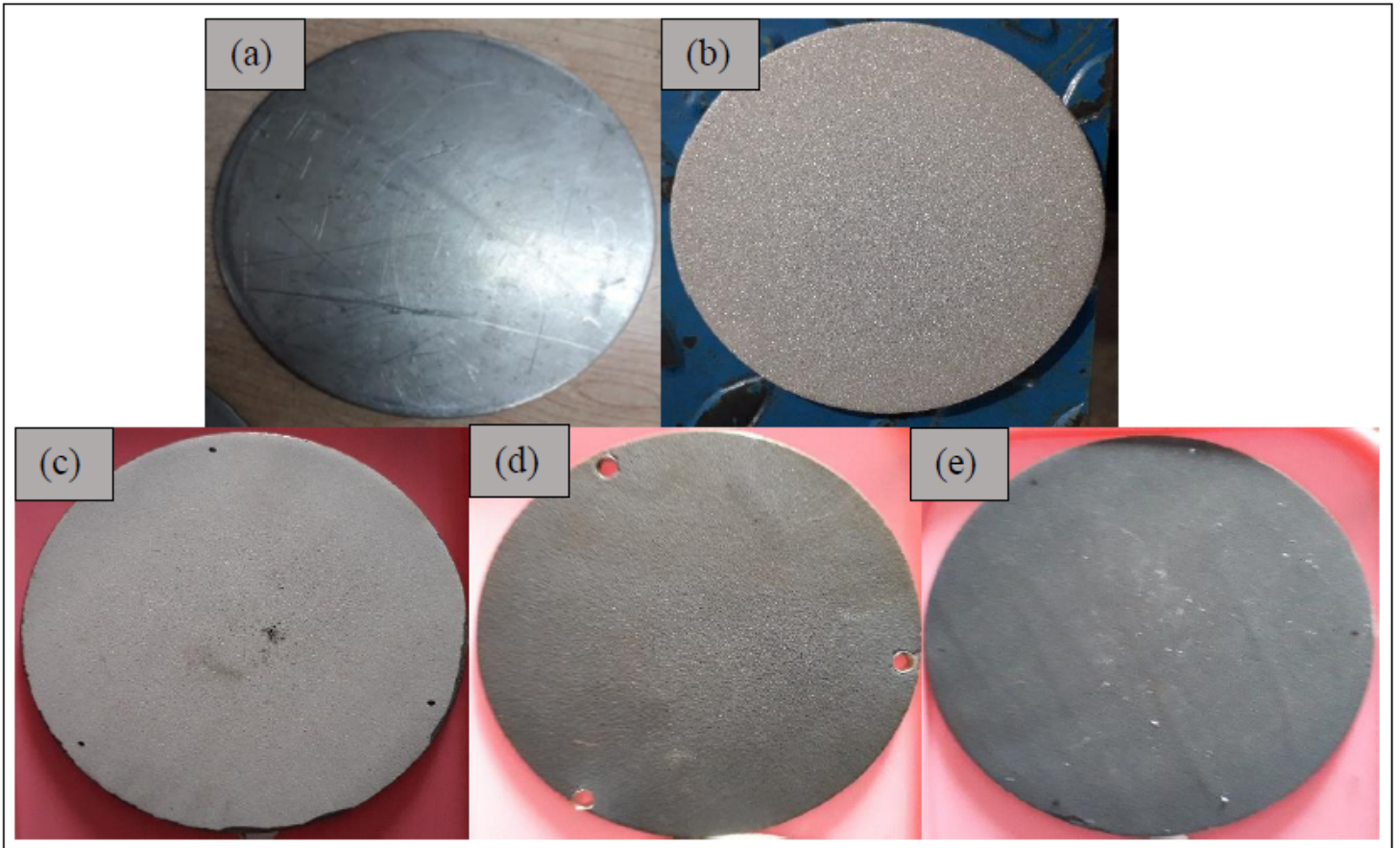


Figure 2

Images of substrate (a) uncoated (b) after alumina grit blasted (c) Al₂O₃ coating (d) Al₂O₃ -13% coating and (e) Al₂O₃ -40% coating substrate.

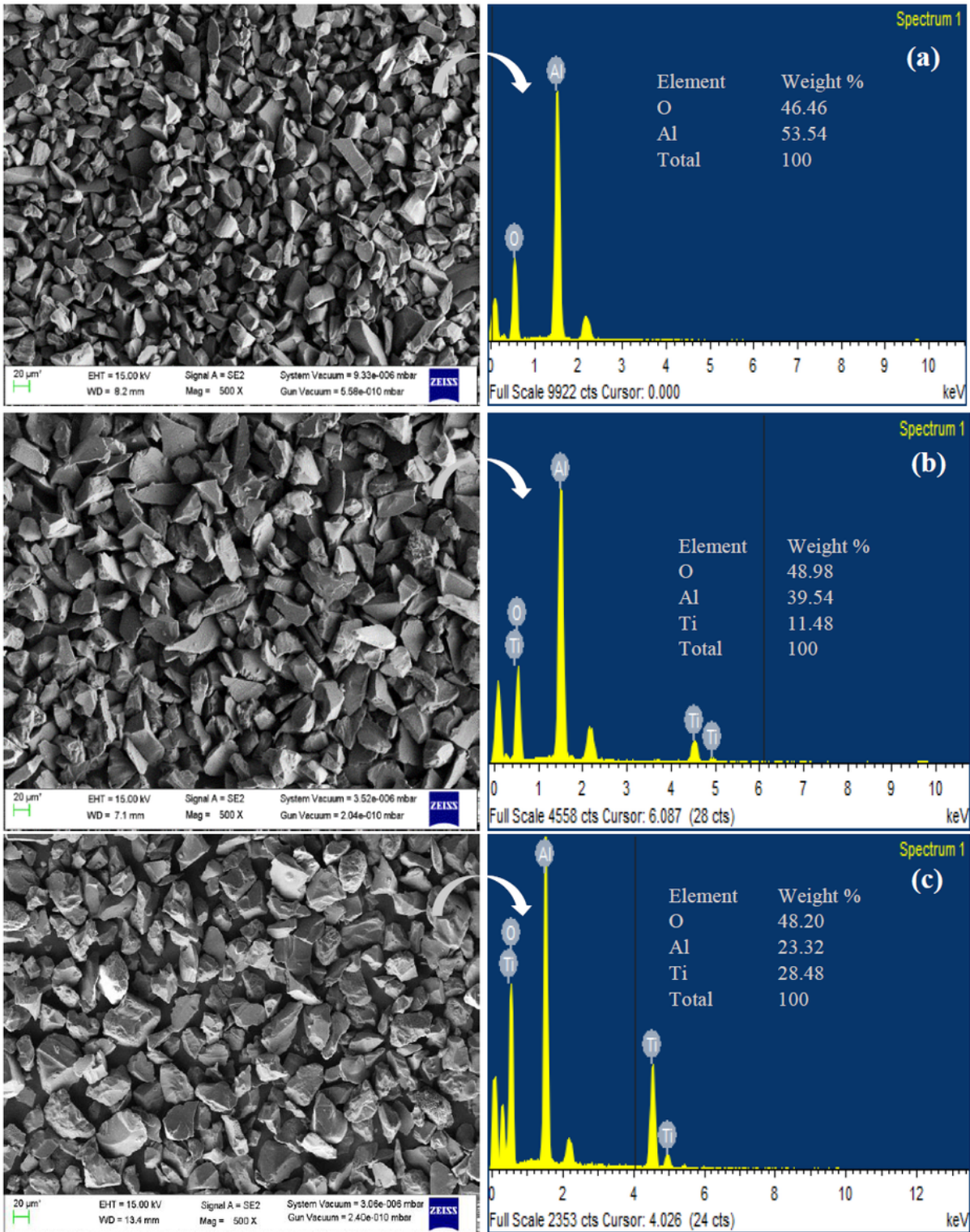


Figure 3

FESEM and EDS analysis of powders (a) Al₂O₃ (b) Al₂O₃ -13% (TiO₂) and (c) Al₂O₃ - 40%(TiO₂).

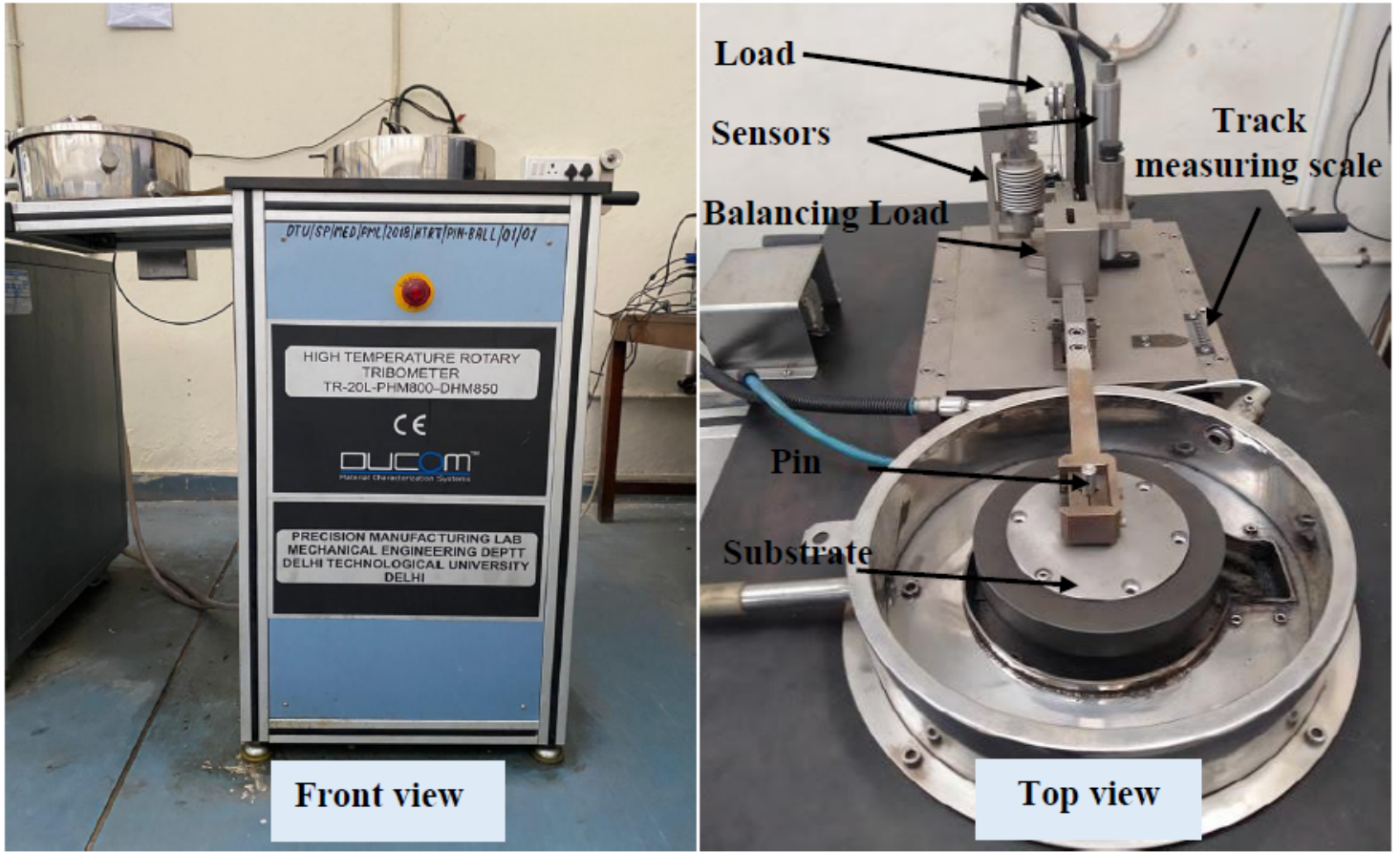


Figure 4

High temperature tribometer setup

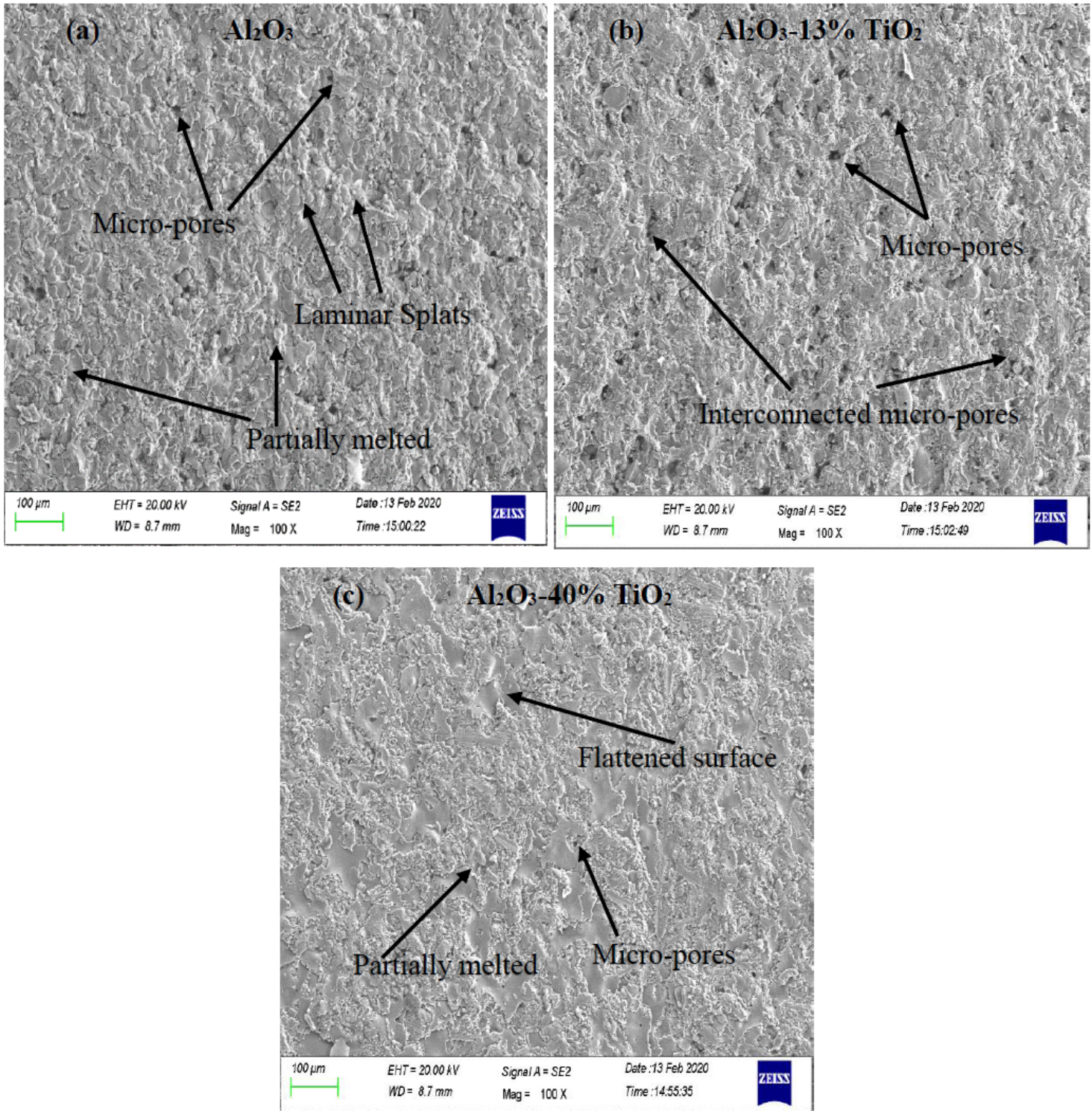


Figure 5

Coating Characterizations: (a) Al_2O_3 coating (b) Al_2O_3 -13% (TiO_2) coating and (c) Al_2O_3 -40% (TiO_2) coating.

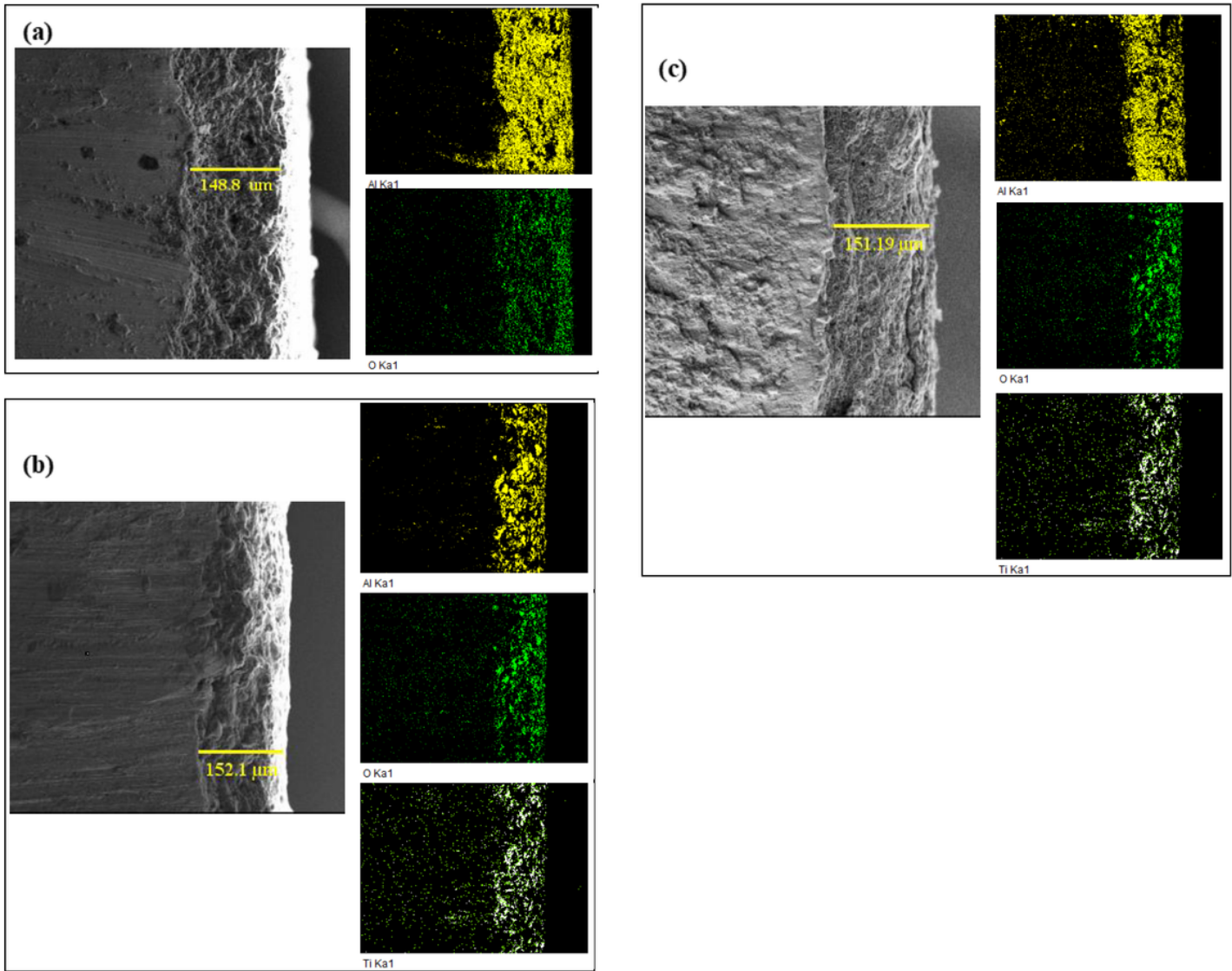


Figure 6

FESEM micrographs and element mapping micrographs of coating thickness (a) Al₂O₃, (b) Al₂O₃ -13% (TiO₂) and (c) Al₂O₃ -40%(TiO₂).

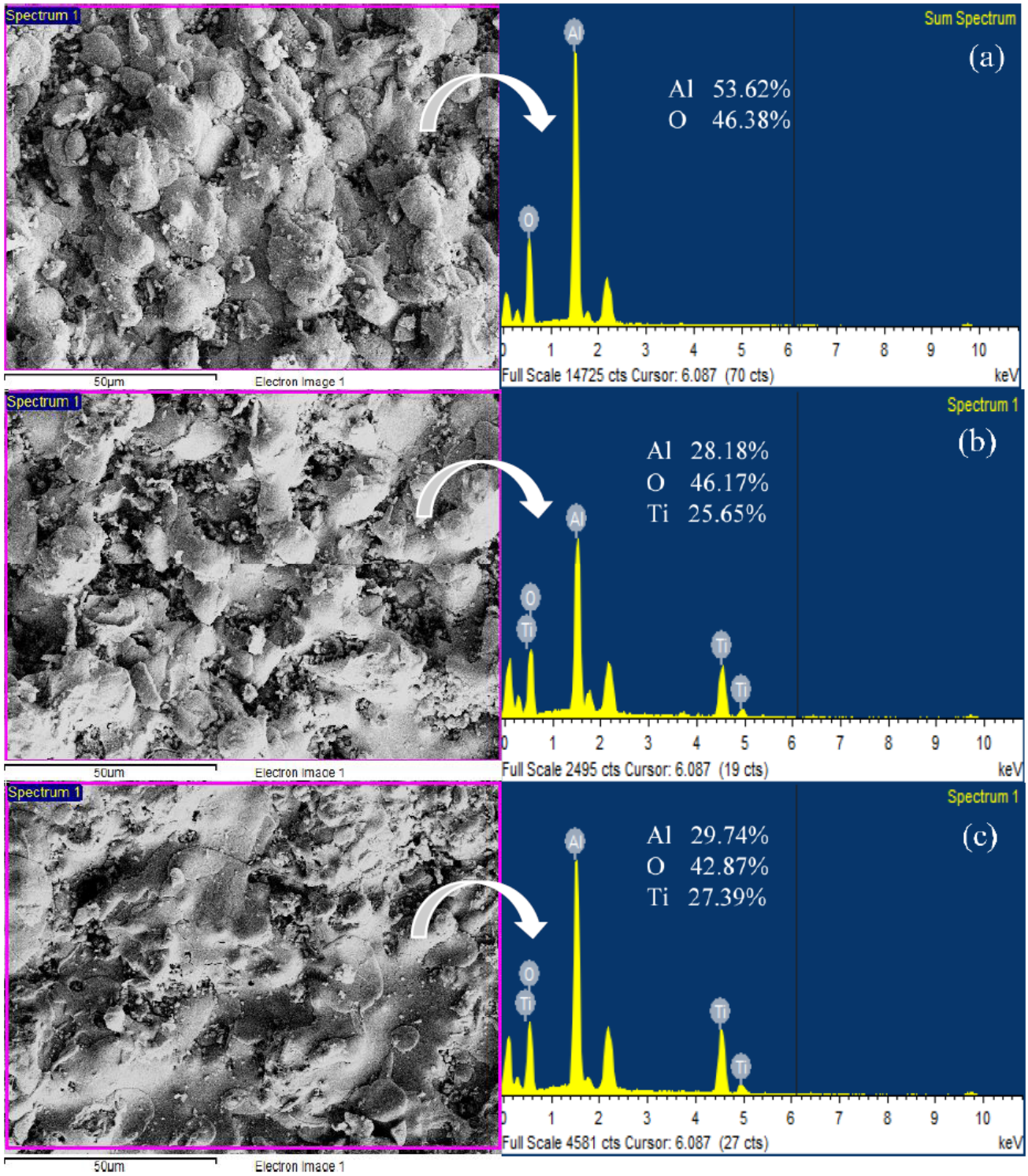


Figure 7

EDS analysis of the coatings (a) Al₂O₃ (b) Al₂O₃-13%(TiO₂) and (c) Al₂O₃-40%(TiO₂).

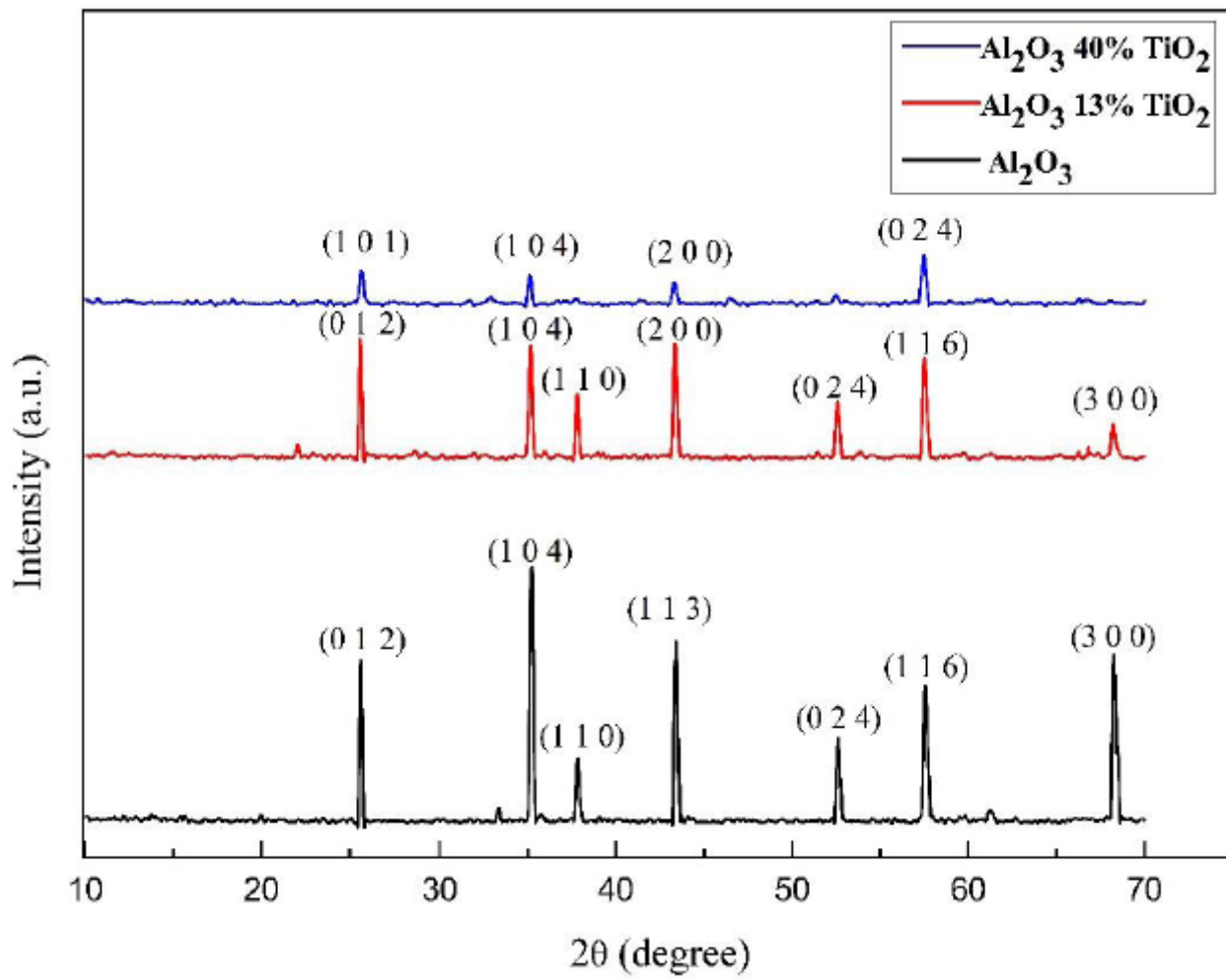


Figure 8

XRD pattern of the deposited coatings.

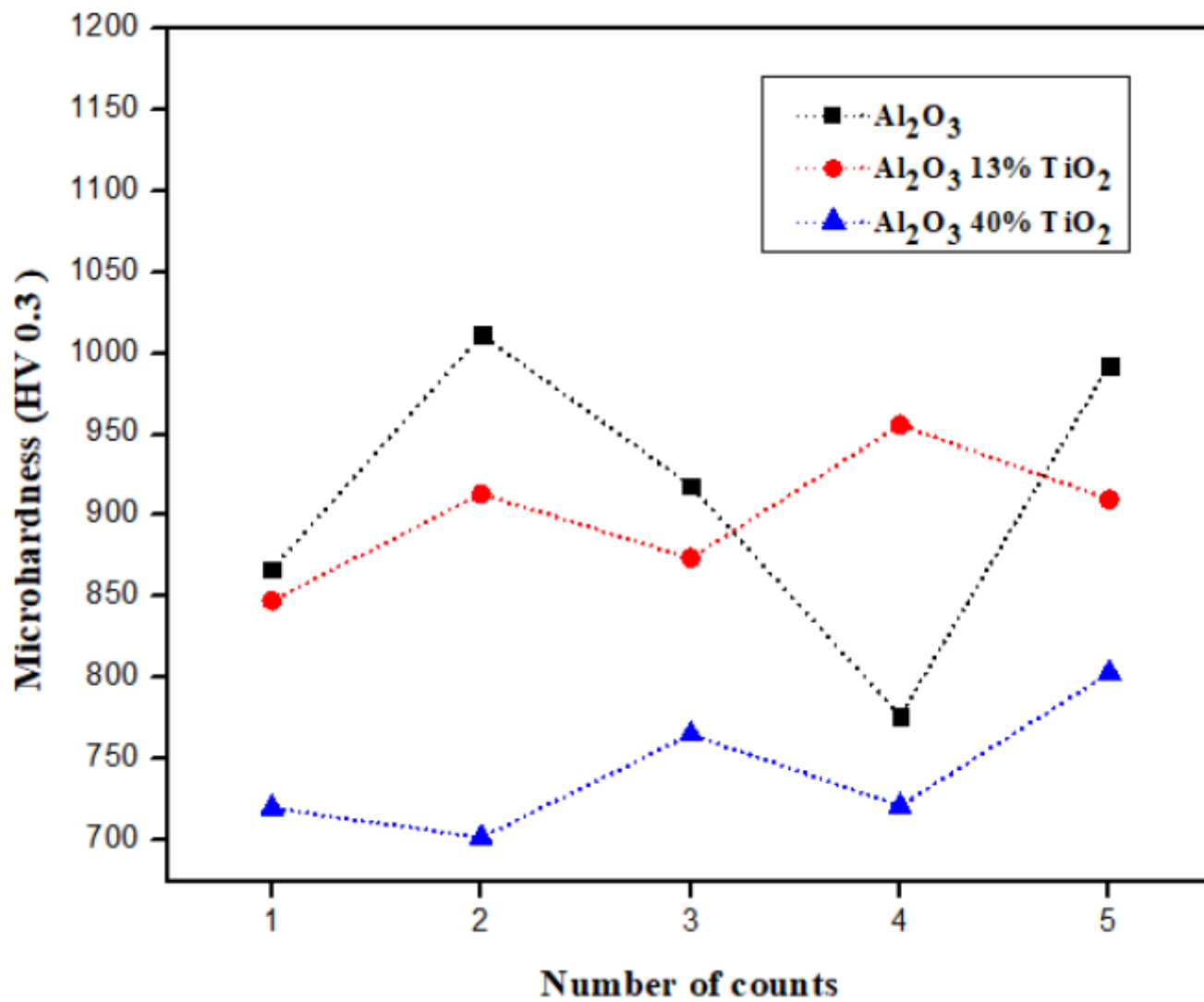


Figure 9

Microhardness graph of the deposited coatings.

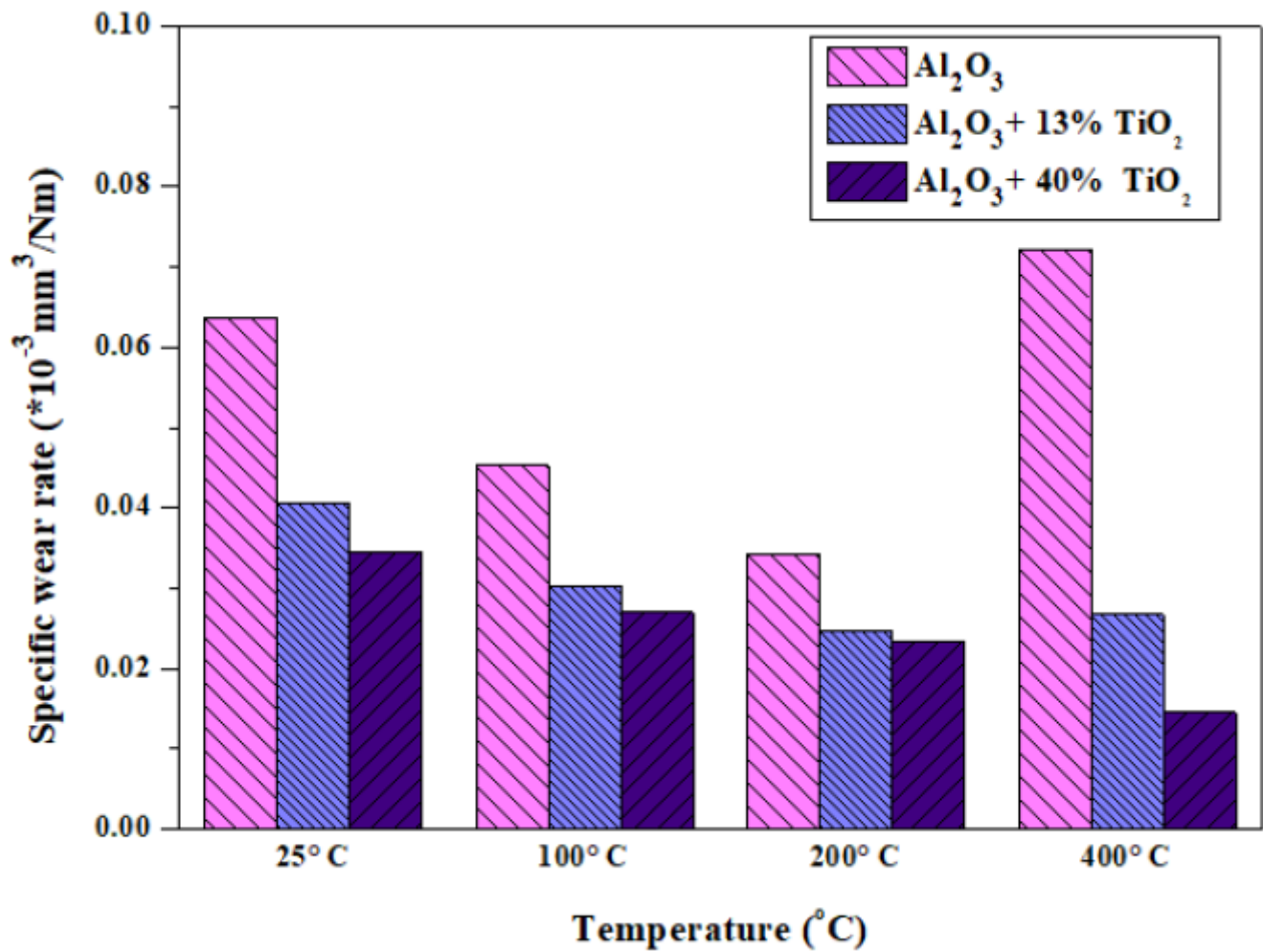


Figure 10

Specific wear rate at different temperature.

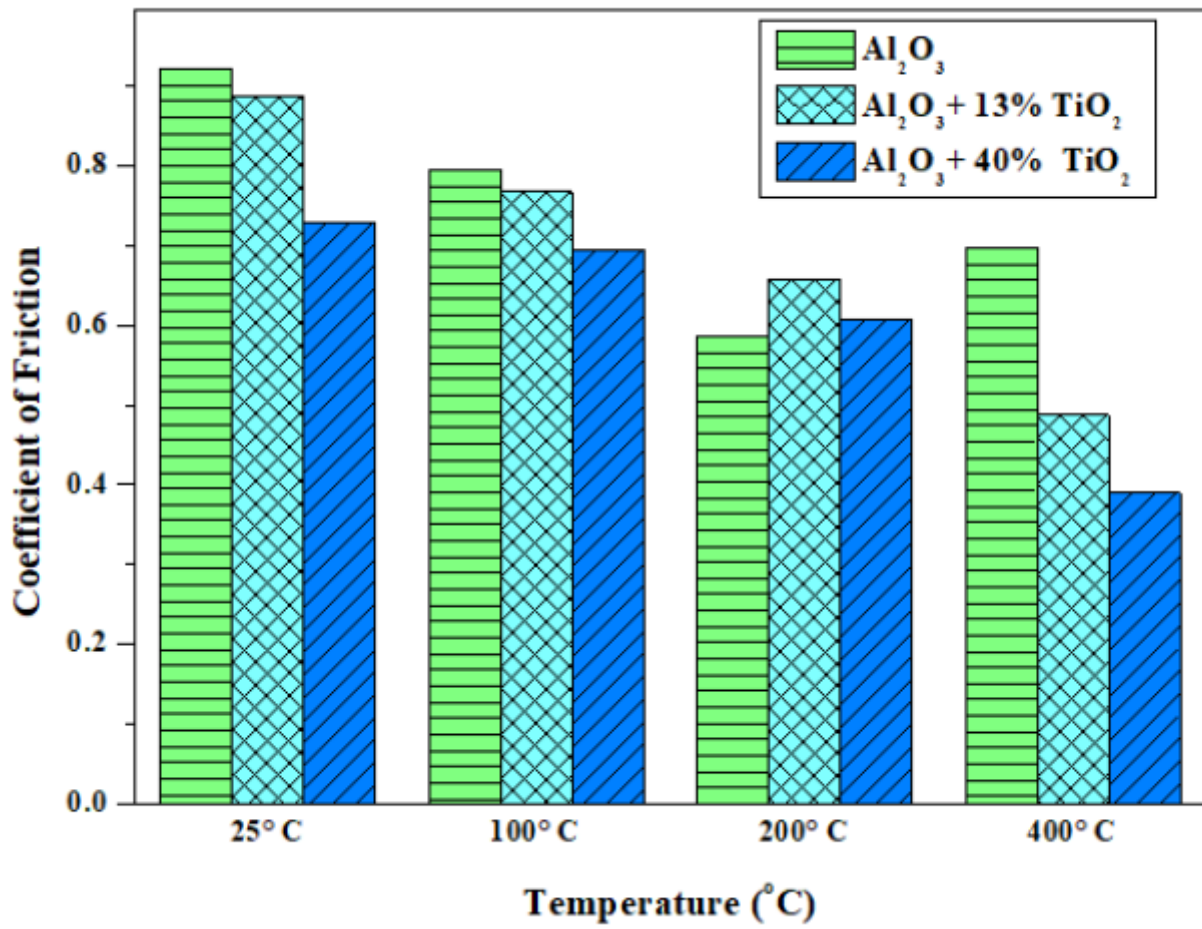


Figure 11

Coefficient of friction at different temperature.

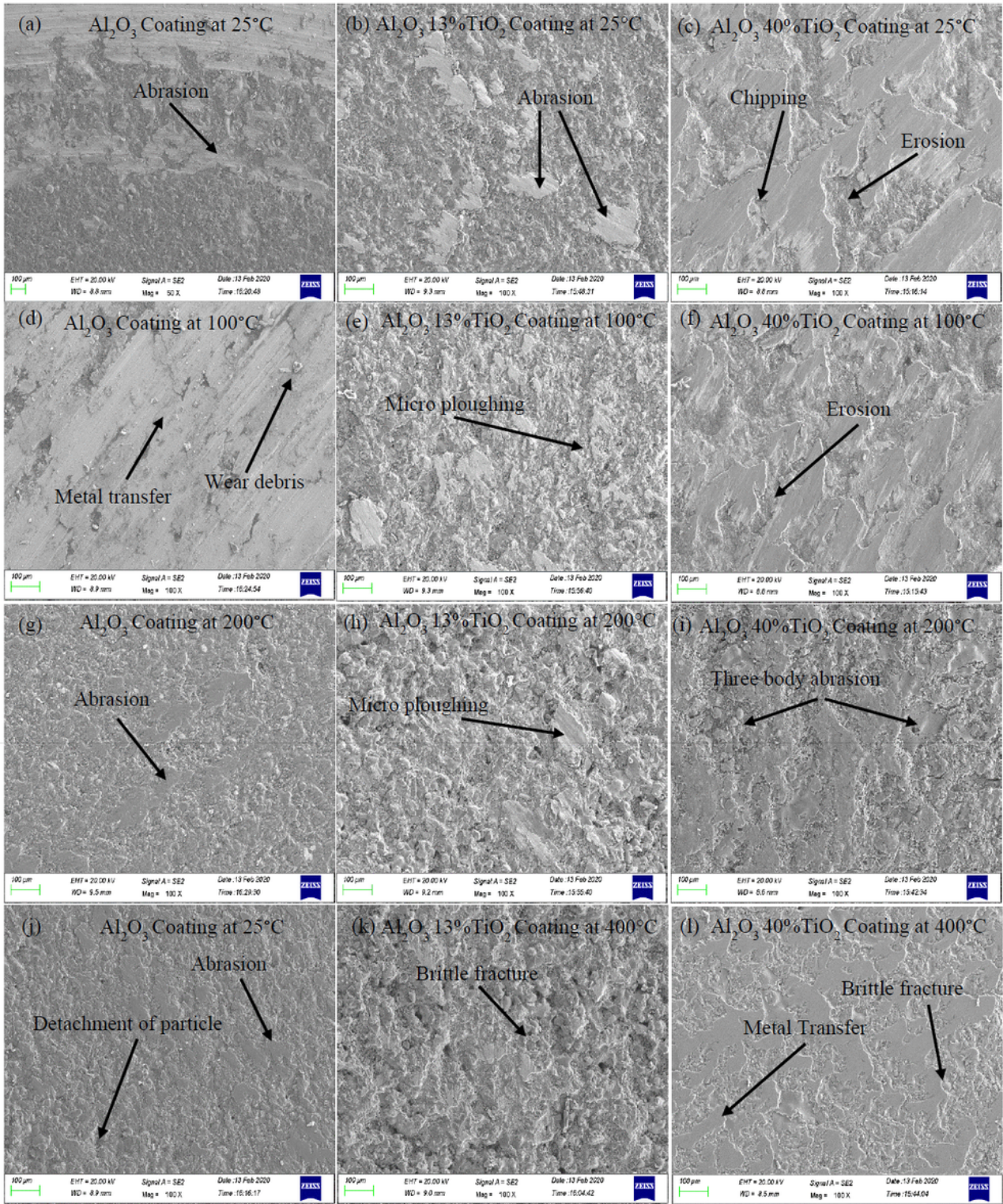


Figure 12

Wear mechanism of the deposited coatings at different temperature.